

# Green chemistry assisted nanoscale synthesis and structural characterization of some transition metal cations

Mustafa Küyükoğlu<sup>1</sup>, Melda Bolat Bülter<sup>2</sup>, Dursun Ali Köse<sup>1,\*</sup>

<sup>1</sup> Hitit University, Department of Chemistry, Ulukavak, Çorum/Türkiye, 19100, ORCID: 0000-0003-4767-6799

<sup>2</sup> Hitit University, Vocational School of Technical Sciences, OHS Program, Çorum/Turkey, 19100

## ABSTRACT

Nanoparticle studies are groundbreaking today, largely due to unpredictable changes in particle size and surface properties. Therefore, nanoparticles are considered as building blocks in optoelectronics, pharmaceuticals, nuclear energy, bioengineering, biomedicine and industrial applications. Today, the importance of environmentally friendly methods is increasing. The use of the green synthesis method, which adopts an economic synthesis approach that will reduce resource and energy consumption and do not harm the environment, is also encouraged in every field. In the study, biosafe ascorbic acid was used as an alternative reagent (agent) to the chemical reduction method. The method process performed with the reagent selected for nanoparticle synthesis has ensured that it is green synthesis, which is adopted as non-toxic and environmentally friendly. In this study, nanoparticles were synthesized by reducing the sulphate, nitrate, chloride and acetate salts of Cu(II), Ni(II), Co(II), Zn(II) and Mn(II) transition metals with the reducing agent ascorbic acid compound. It is aimed to investigate the effects of the same metal cations and different anion salts on nanoparticle synthesis. Depending on the radius ratios and solubility values of metal cations and anions, the nanoparticle obtained from Ni(CH<sub>3</sub>COO)<sub>2</sub> salt has the smallest radius. Nano metal particles with the largest radius were obtained as a result of reduction from Co(NO<sub>3</sub>)<sub>2</sub> salt. The characterization of the synthesized nanoparticles were recorded by particle size analysis and scanning electron microscopy (SEM) images.

## ARTICLE INFO

### Research article

Received: 10.04.2023

Accepted: 16.05.2023

### Keywords:

Transition metal,  
cation,  
nanoparticle,  
ascorbic acid,  
reduction

\*Corresponding author

## 1. Introduction

Nanotechnology is a science that deals with the preparation of nano-sized particles ranging from 1 to 100 nm using various synthesis strategies and particle structure and size modification. Nanoparticles have proven to be a scientific and technological boon that can be used in many different application areas such as medicine, organic chemistry, inorganic chemistry, materials science, food, electronics, fuel cells, solar cells, voltaic batteries, chemical sensors, space, sports equipment, chemical fabrics [1-9]. Due to the specific properties (size, shape, and distribution) of nanoparticles, they can be used in applications requiring advanced technology [10-12]. Nanoparticles of transition metals also have wide applications in different interdisciplinary fields due to their distinctive physicochemical properties associated with their nanometer size [5-8]. Metal oxide nanoparticles (MONs) are synthesized from all-metal precursors. These nanoparticles play an important role in many fields of physics, chemistry, and materials science. MONs have unique optoelectrical

properties due to their well-known localized surface plasmon resonance properties. Nano-sized metal oxides have many outstanding properties, including high cleaning capacity and heavy metal selectivity. They hold great potential as promising adsorbents for heavy metals. Therefore, synthesis techniques mainly focus on size, morphological configuration, stability, and distribution [17-21]. The chemicals used for nanoparticle synthesis and stabilization are toxic and lead to non-biosafe by-products. Therefore, there is a growing interest in “green nanotechnology” that is environmentally friendly with the specific properties of nanoparticles [22-25]. The reduction of metal nanoparticles with the ascorbic acid compound can be said to be a green method whose process is non-toxic, low cost, and environmentally friendly [10,26-31]. When the transition metal studies in the literature are examined, it is seen that there is a focus on certain transition metals. In this study, sulphate, nitrate, chloride, and acetate salts of Cu(II), Ni(II), Co(II), Zn(II), and Mn(II) transition metal cations were combined with L-ascorbic acid (Vitamin C) using chemical reduction technique. nanoscale syntheses

were tried to be made by reducing. Thus, it is aimed to investigate the effects of the same metal cations with different anion salts on nanoparticle synthesis. The synthesis of MON and anion and their effects on size will be examined. It is aimed to create a reference source for researches aiming to study nano-sized particles of specified metal cations. ZETA particle size analysis and scanning electron microscope (SEM) images were recorded for the characterization of the synthesized nanoparticles.

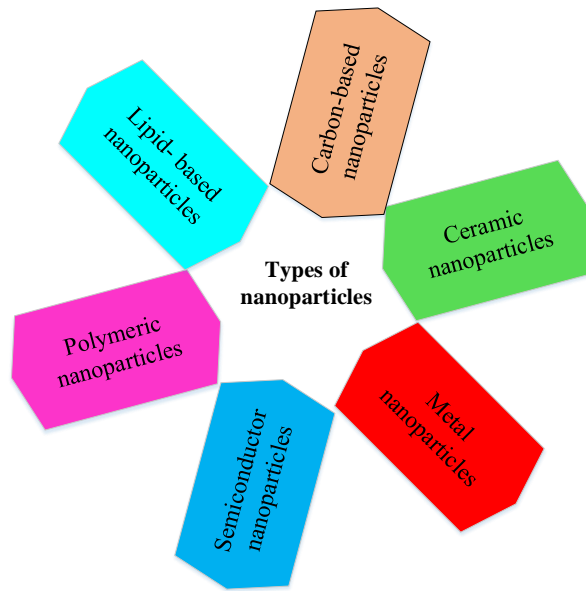


**Figure 1.** Commonly used types of nanoparticles [32]

## 2. Materials and methods

### 2.1. Materials

Sulfate, nitrate, chloride and acetate salts of copper, nickel, cobalt, zinc and manganese and ascorbic acid chemicals were procured from Sigma-Aldrich (St. Louis, USA). All other

chemicals used in the study are of analytical grade. De-ionized water was also used in the study.

### 2.2. Synthesis of transition metal nanoparticles

In this study, metal oxide nanoparticle synthesis was performed as follows. 0.001 mol of transition metal salt and 0.011 mol of ascorbic acid were dissolved in 100 mL of de-ionized water. The pH of the solution was brought to about 6.50 with NaOH solution. The solution was then taken into a flask and placed in the assembly consisting of a water bath and a mechanical stirrer. The transition metal solution was stirred for 2.5 hours at 85°C, 700 rpm. In the last stage, the large particles and unwanted impurities settled to the bottom were filtered under vacuum and the metal nanoparticle solids remaining at the bottom of the flask after the water were removed by the evaporator device and where dried with a vacuum oven at 25 °C.

### 2.3. Characterization

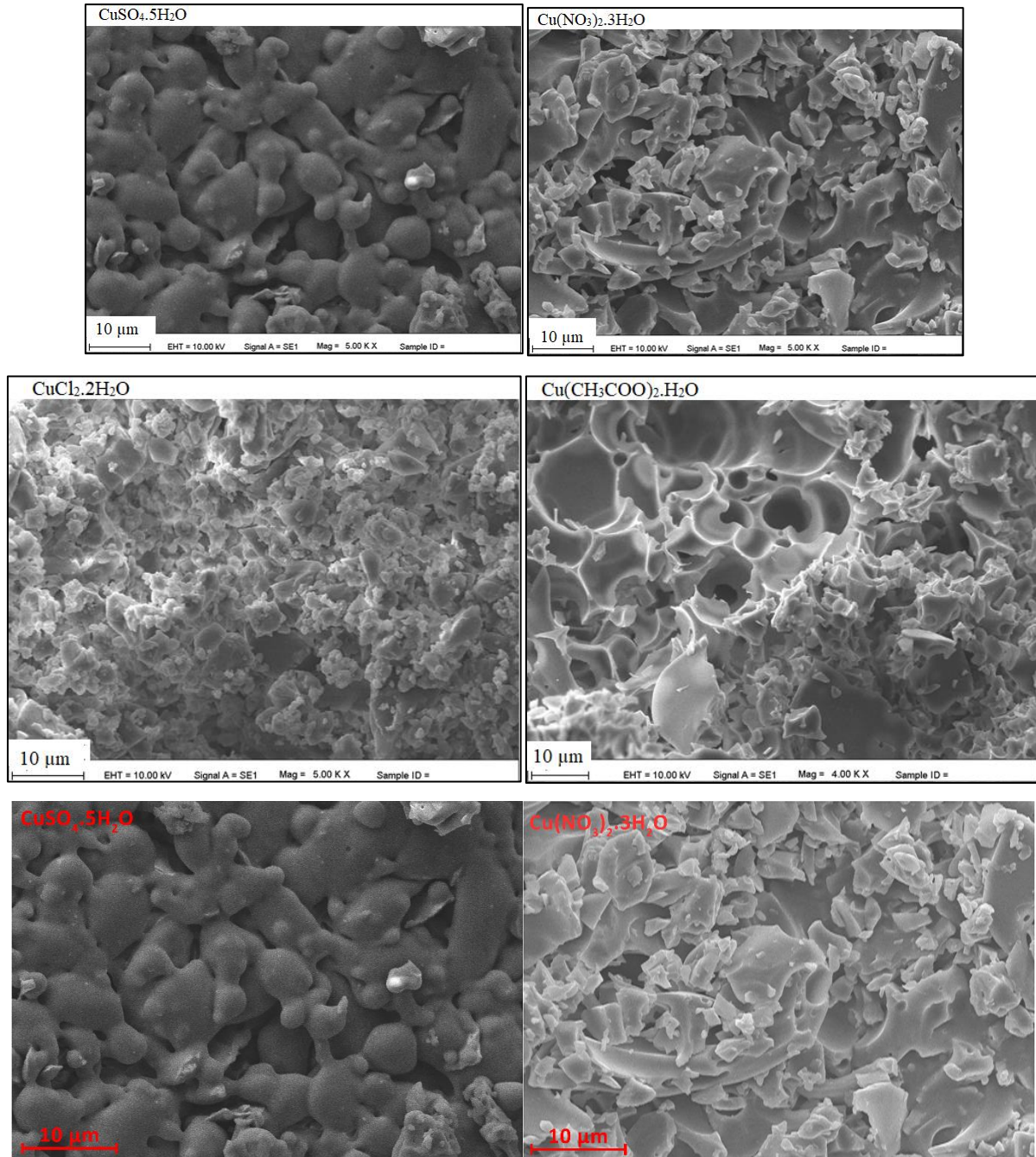
#### Scanning Electron Microscope (SEM)

Surface morphology of the synthesized nanoparticles was investigated using scanning electron microscopy (SEM; FEI / Quanta 450 FEG, USA). The sample, which was attached to the SEM holder with double-sided carbon tape, was then covered under vacuum with a thin layer of gold. Then the obtained SEM sample was placed in the device and its image was taken.

#### Size Analysis

The size of the nanoparticles in the aqueous solution was analyzed. The scattering angle of the laser light passing through the particle depends on the particle size. As the particle size decreases, the scatter angle increases logarithmically. The scattering angles of large particles are low, the intensity of the scattered laser light is high. In small particles, the scattering angle is high and the intensity of the scattered laser light is low.

## 3. Results and discussions

**Scanning Electron Microscopy (SEM)**

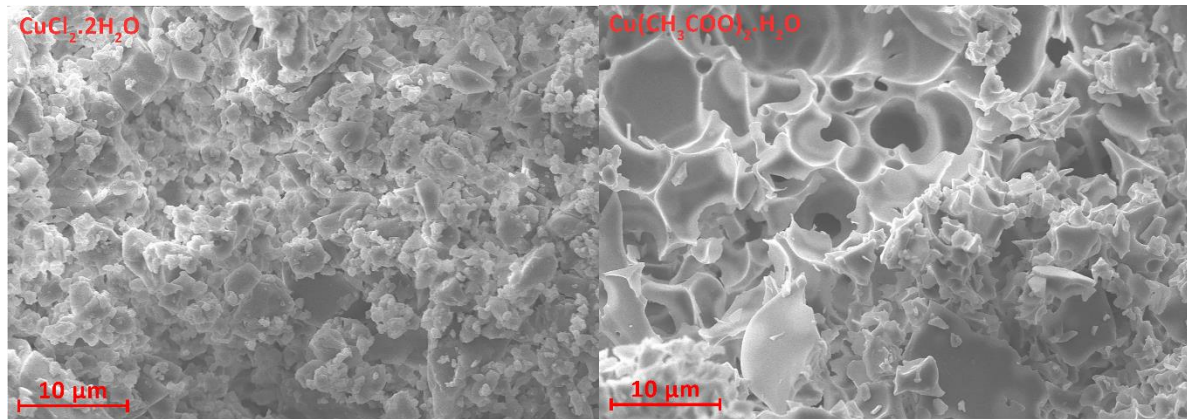
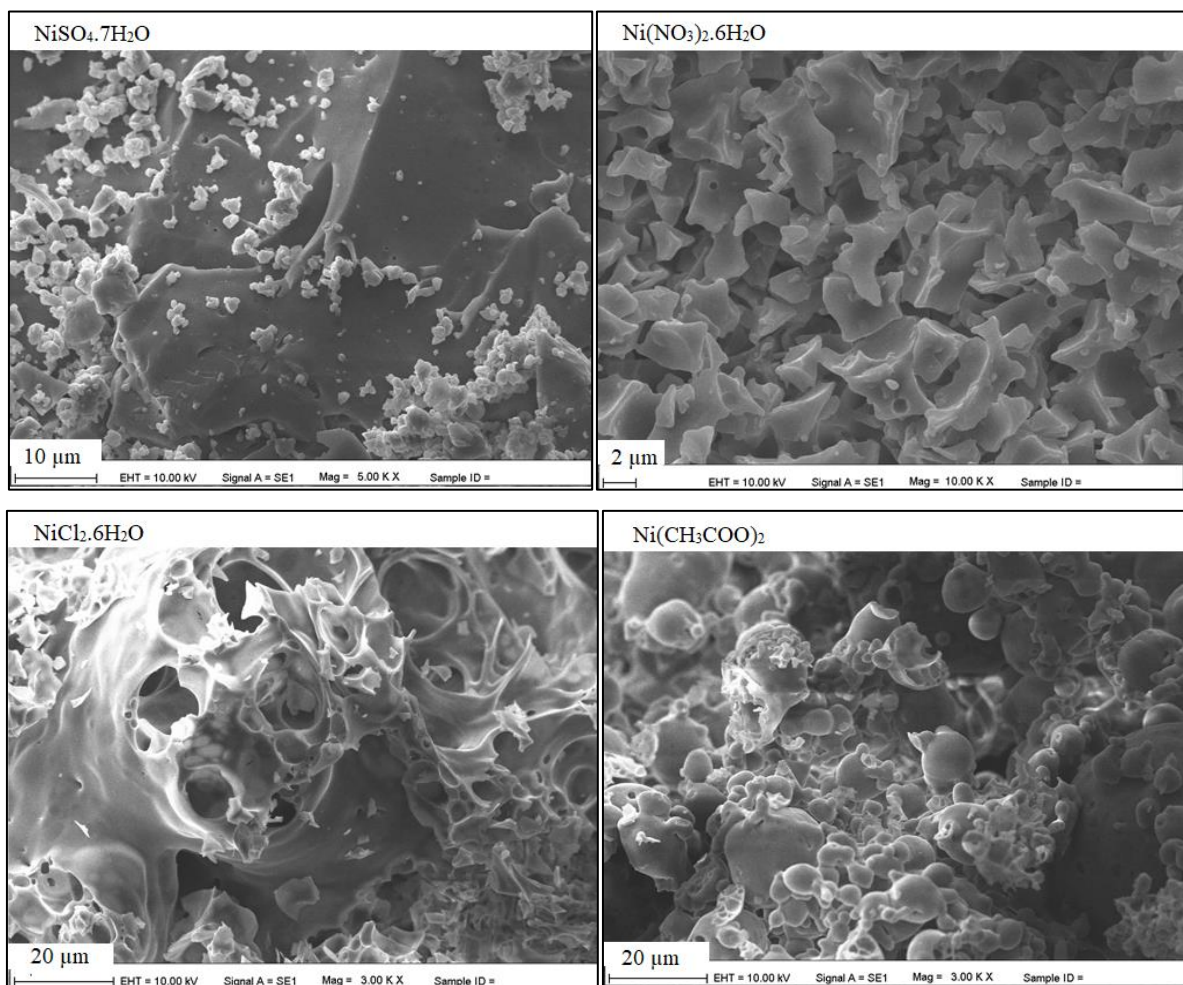


Figure 2. SEM image of nanoparticles obtained from Cu (II) salts



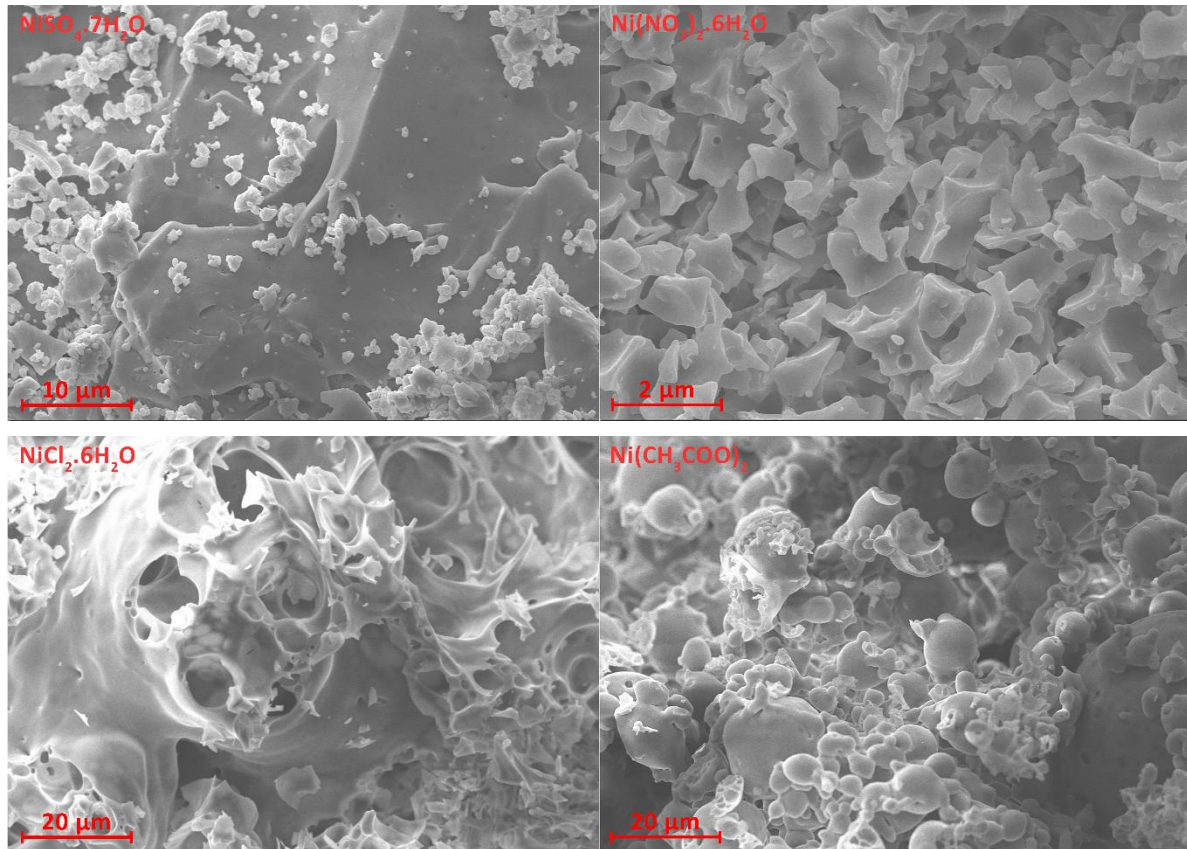
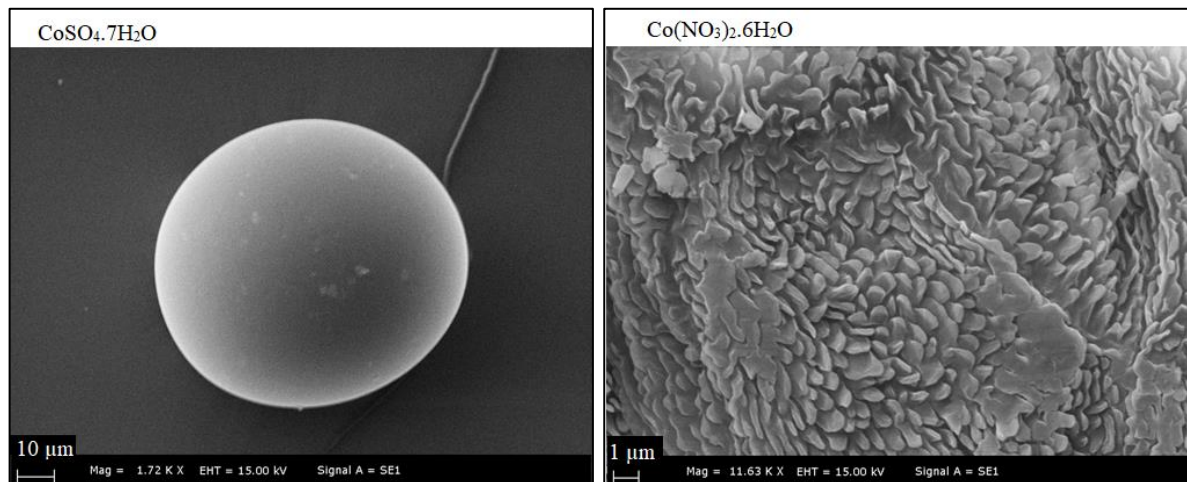


Figure 3. SEM image of nanoparticles obtained from Ni (II) salts



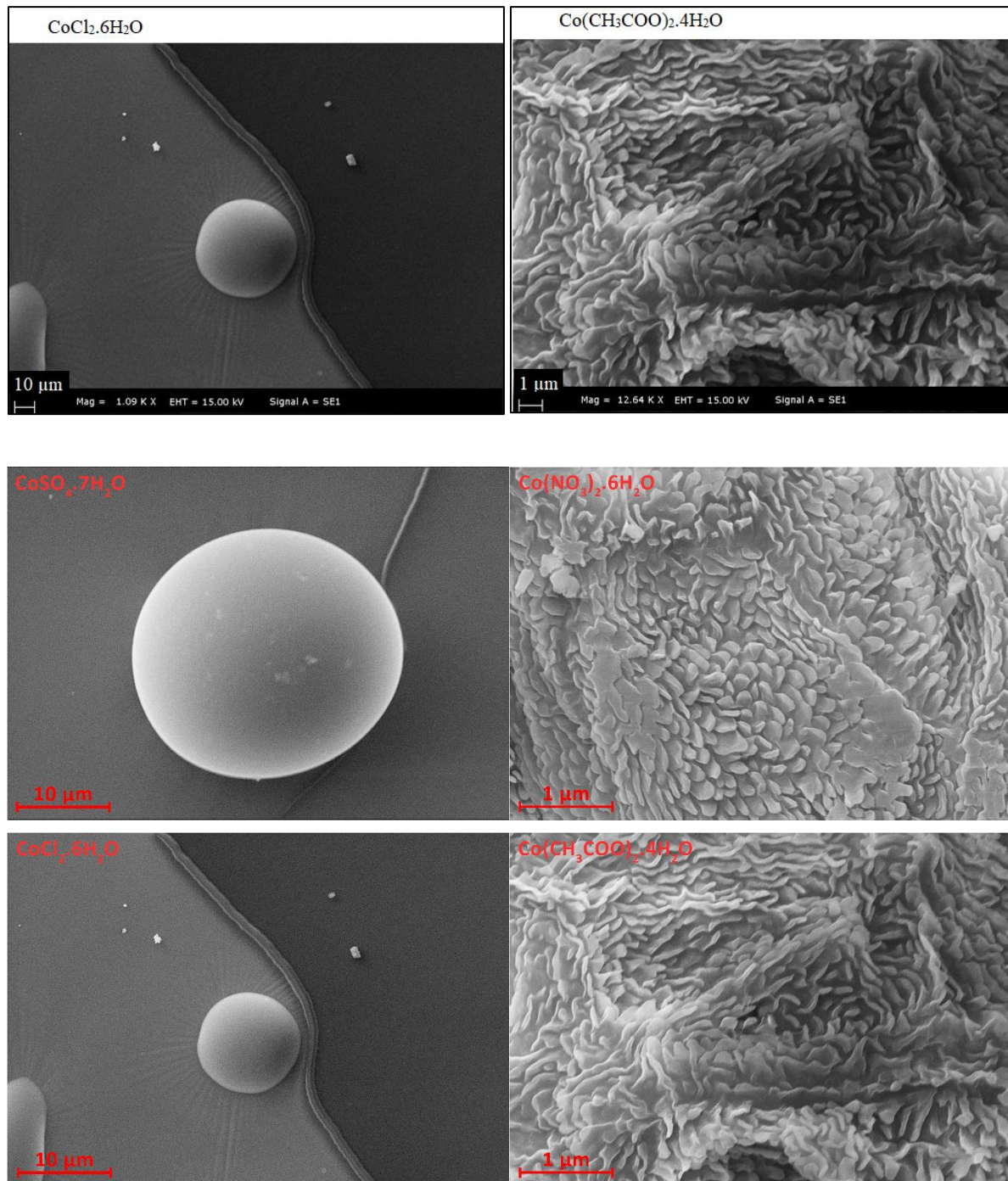
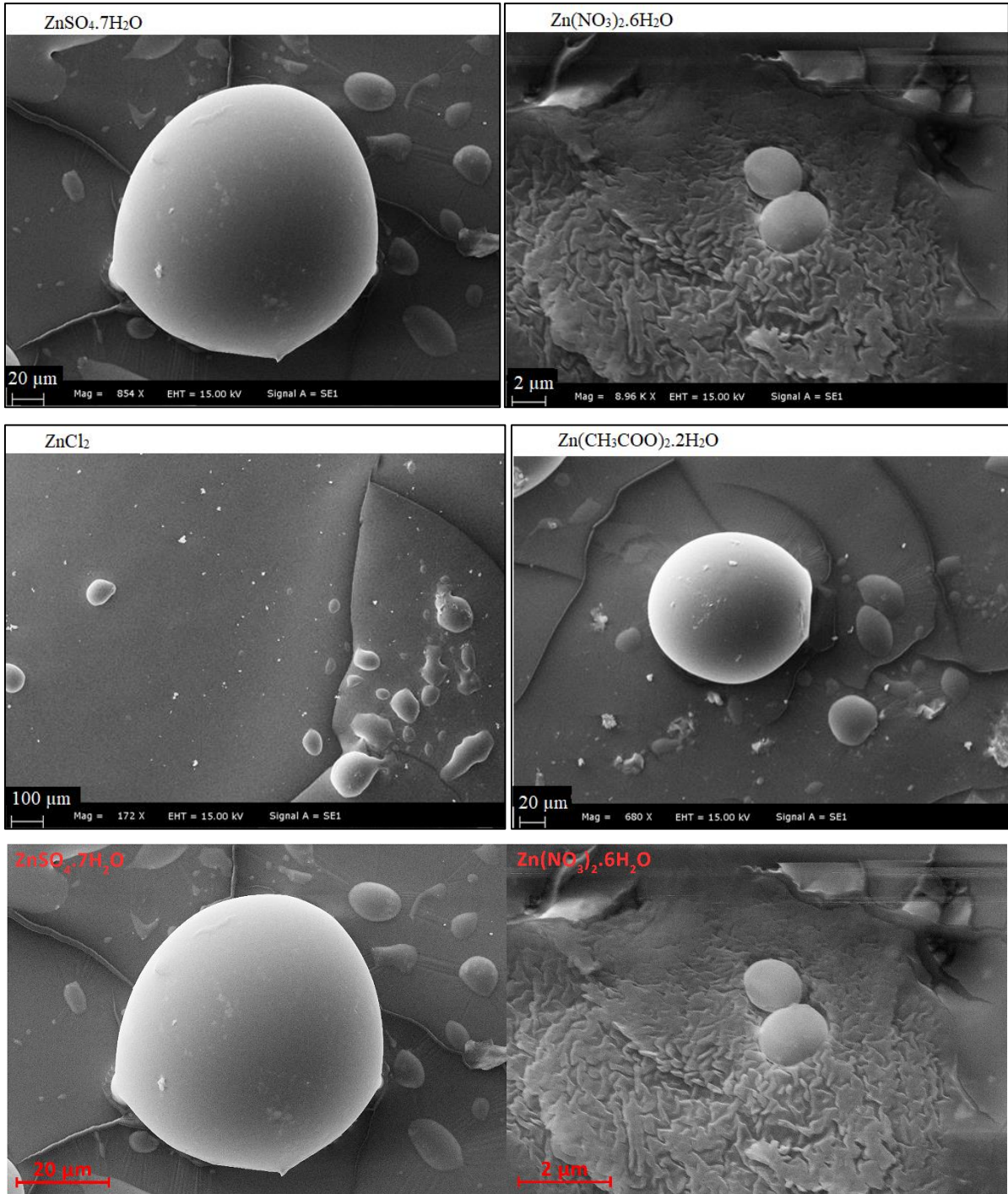


Figure 4. SEM image of nanoparticles obtained from Co (II) salts



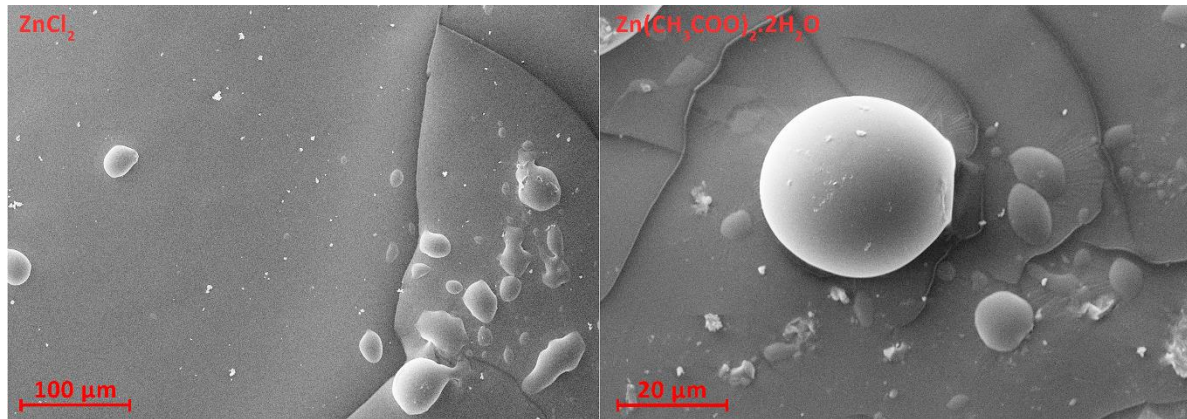
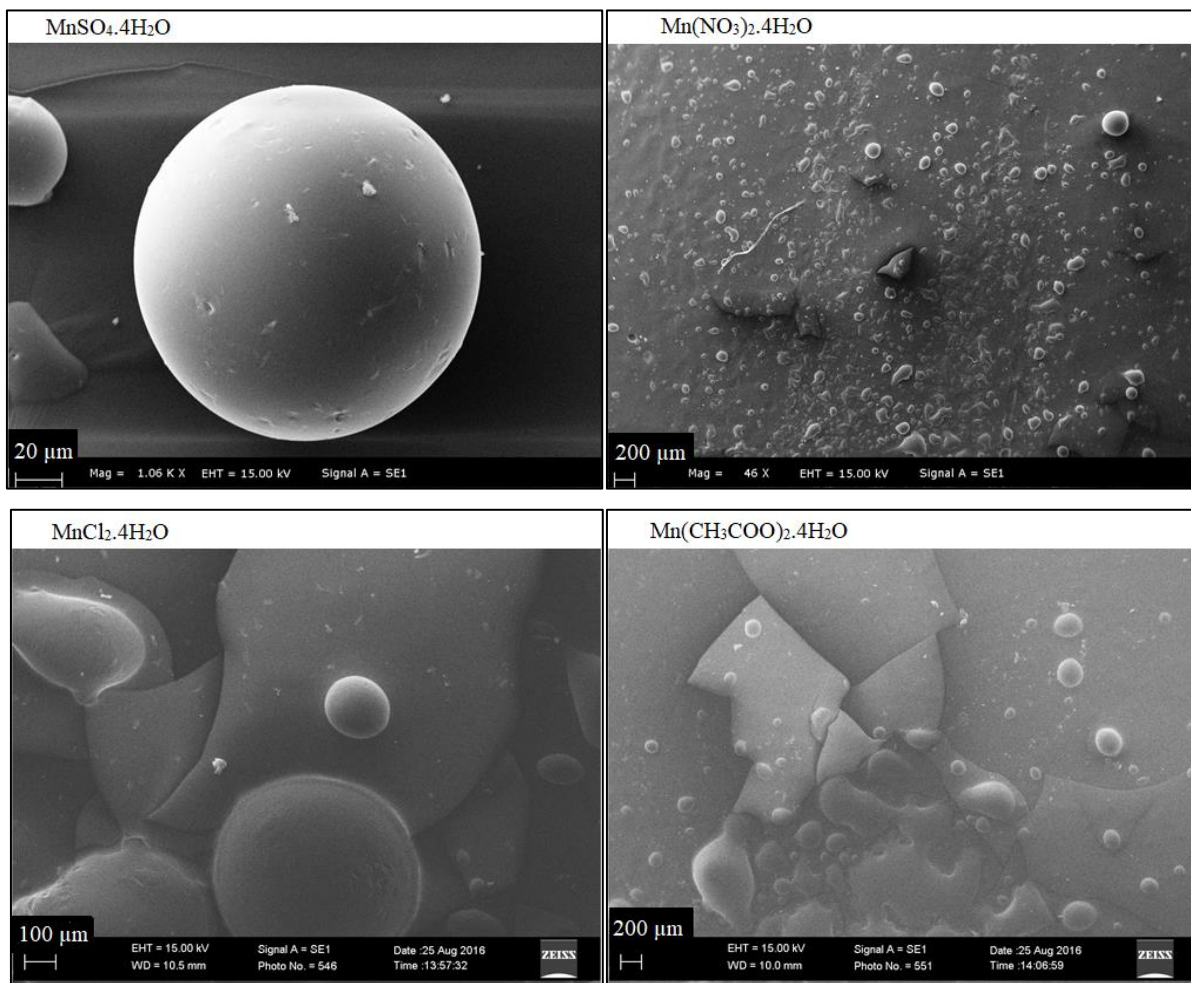
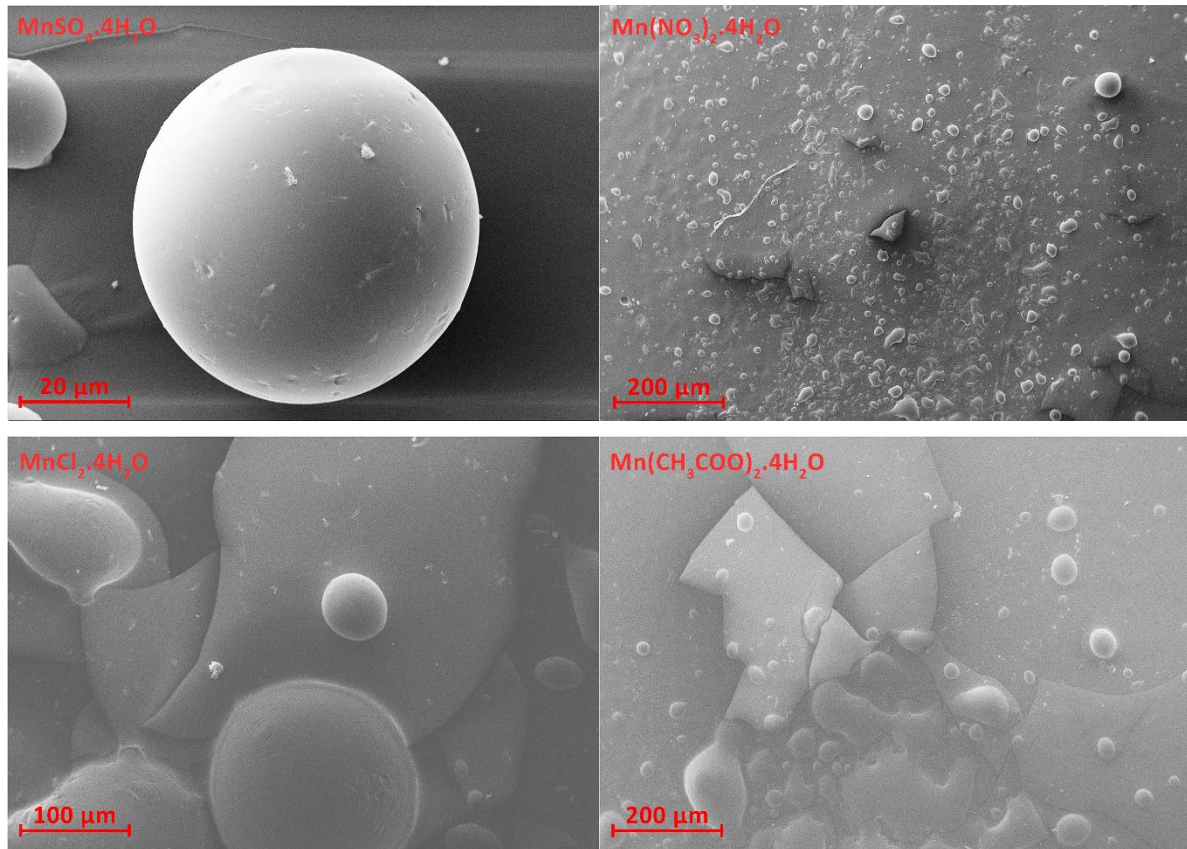


Figure 5. SEM image of nanoparticles obtained from Zn(II) salts





**Figure 6.** SEM image of nanoparticles obtained from Mn(II) salts

Zeta-Size chart

The size of the smallest nanoparticles was determined as  $\text{Ni}(\text{CH}_3\text{COO})_2$  and is shown in figure 7. The largest

nanoparticle was determined as  $\text{Co}(\text{NO}_3)_2 \cdot 6\text{H}_2\text{O}$  and is shown in figure 8.

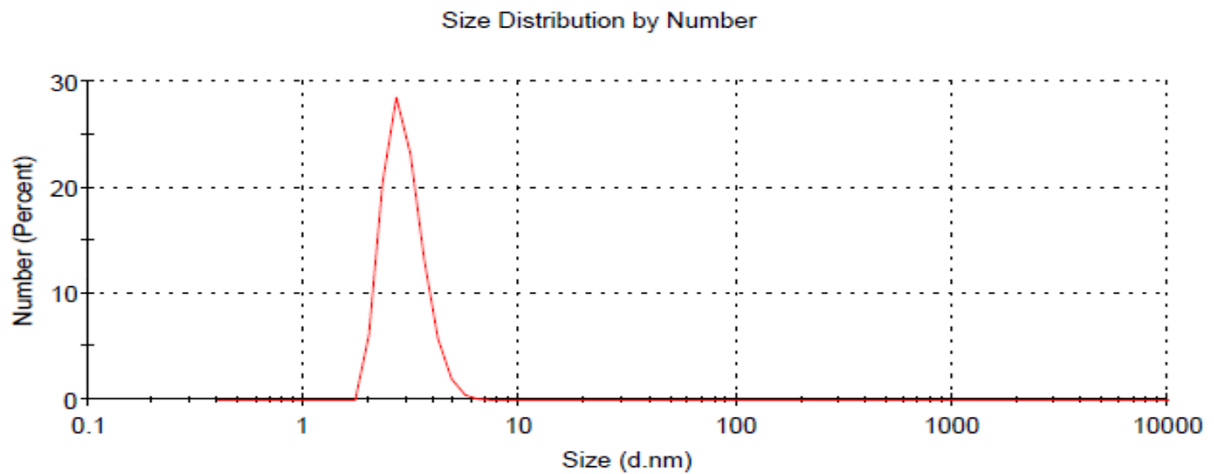


**Figure 7.** Zeta-Size graph of the smallest nanoparticle  $\text{Ni}(\text{CH}_3\text{COO})_2$

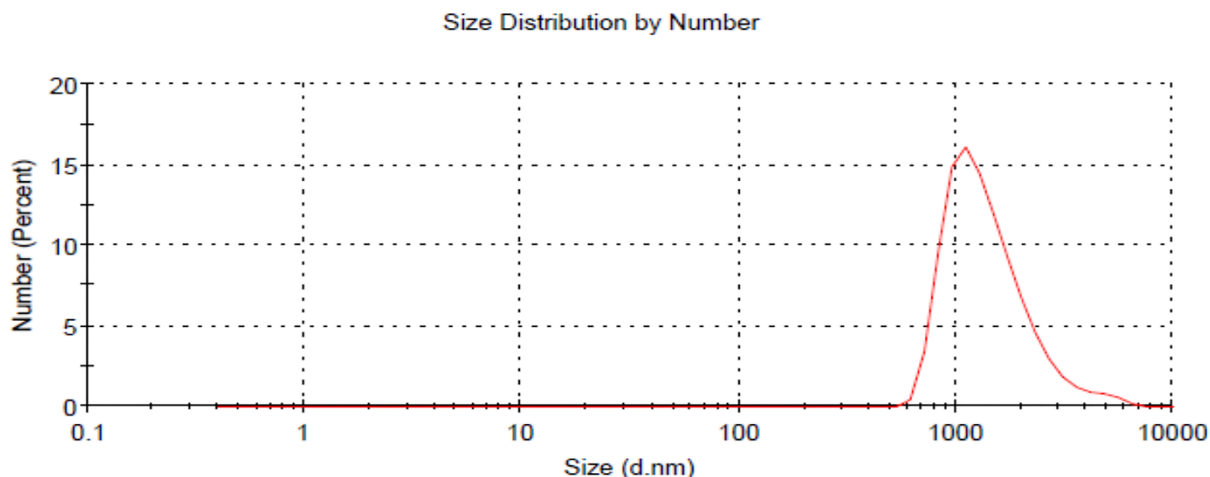


**Figure 8.** Zeta-Size graph of the largest nanoparticle  $\text{Co}(\text{NO}_3)_2 \cdot 6\text{H}_2\text{O}$

**Table 1.** Size analysis of nanoparticles based on anions and cations

Anion	$\text{Cu}^{+2}(\text{nm})$	$\text{Ni}^{2+}(\text{nm})$	$\text{Co}^{+2}(\text{nm})$	$\text{Zn}^{+2}(\text{nm})$	$\text{Mn}^{+2}(\text{nm})$
Sulfate	709,6	310,8	603,9	812,6	718,3
Nitrate	635,9	145,8	1492,0	675,9	118,4
Chloride	3,421	453,7	887,3	645,8	564,4
Acetate	867,4	2,946	615,3	53,03	683,6

In the light of the data summarized in Table 1, when the size analysis of the nanoparticles is examined, the order of the salts used according to the size of the particles obtained from the small to the large is as follows: Among the cations, the smallest particle size was obtained from Ni (II) salts. It has been determined that salts with the smallest size acetate anion are formed among the anions. Accordingly, it can be said that the low solubility of nickel acetate in aqueous environment

General Ranking:

$\text{Ni}(\text{CH}_3\text{COO})_2 < \text{CuCl}_2 < \text{Zn}(\text{CH}_3\text{COO})_2 < \text{Mn}(\text{NO}_3)_2 < \text{Ni}(\text{NO}_3)_2 < \text{NiSO}_4 < \text{NiCl}_2 < \text{MnCl}_2 < \text{CoSO}_4 < \text{Co}(\text{CH}_3\text{COO})_2 < \text{Cu}(\text{NO}_3)_2 < \text{ZnCl}_2 < \text{Zn}(\text{NO}_3)_2 < \text{Mn}(\text{CH}_3\text{COO})_2 < \text{CuSO}_4 < \text{MnSO}_4 < \text{ZnSO}_4 < \text{Cu}(\text{CH}_3\text{COO})_2 < \text{CoCl}_2 < \text{Co}(\text{NO}_3)_2$

When the anion-based size analysis is examined, the following sequence is formed from small to large.

Anion Rank:  $\text{CH}_3\text{COO}^- < \text{Cl}^- < \text{NO}_3^- < \text{SO}_4^{2-}$

When the cation based size analysis is examined, the following sequence is formed from small to large.

Cation Rank:  $\text{Ni}^{2+} < \text{Mn}^{2+} < \text{Zn}^{2+} < \text{Cu}^{2+} < \text{Co}^{2+}$

When the radius values of the anions given in Table 2 are examined, it has been determined that the largest radius value is  $\text{SO}_4^{2-}$  anion and the lowest value is  $\text{CH}_3\text{COO}^-$

compared to other salts caused the nanoparticles obtained to be smaller in size. Based on the same idea, the cobalt nitrate salt, which dissolves relatively faster in an aqueous environment, has also been identified as the largest particle. According to the results of the size analysis, the general comparisons of the particles formed by the reduction of the salts with ascorbic acid are shown below.

In Table 3, the radius values of the metal cations with 2+ oxidation steps are close to each other, as expected, the small value is  $\text{Co}^{2+}$  with low spin, and the highest value is the  $\text{Zn}^{2+}$  cation with d10 electronic configuration.  $\text{Mn}^{2+}$  d5 deviates from the periodic table bases since it has a half-filled stability electronic configuration at varying radii in accordance with the periodic table rules.

**Table 2.** The radius values of anions [33]

Anion	Radius (nm)	Cu <sup>2+</sup>	73
CH <sub>3</sub> COO <sup>-</sup>	162	Mn <sup>2+</sup>	81(ls) 97 (hs)
NO <sub>3</sub> <sup>-</sup>	179	Ni <sup>2+</sup>	83
Cl <sup>-</sup>	184	Zn <sup>2+</sup>	88
SO <sub>4</sub> <sup>2-</sup>	258	ls: low spin, hs: high spin	

**Table 3.** The radius values of anions [34]

Cation	Radius(pm)
Co <sup>2+</sup>	65 (ls) 74,5 (hs)

When the solubilities of metal salts consisting of cations and anions are compared, the solubility decreases in ionic compounds (salt compounds) formed by cations and anions whose radii are close to each other due to the increasing covalent character feature. When the solubility values of the metal salts given as g/mL in an aqueous medium at 20oC in Table 4 are examined, they show the expected changes (due to periodic table exceptions), albeit small deviations.

**Table 4.** The solubility values of the metal salts.

Metal Salt	Solubility (g/100mL, 20°C)
Zn(CH <sub>3</sub> COO) <sub>2</sub> .2H <sub>2</sub> O	43.0
Zn(NO <sub>3</sub> ) <sub>2</sub> .6H <sub>2</sub> O	184.0
ZnSO <sub>4</sub> .7H <sub>2</sub> O	96.0
ZnCl <sub>2</sub>	395.0
Cu(CH <sub>3</sub> COO) <sub>2</sub> .H <sub>2</sub> O	7.2
Cu(NO <sub>3</sub> ) <sub>2</sub> .3H <sub>2</sub> O	125.0
CuSO <sub>4</sub> .5H <sub>2</sub> O	32.0
CuCl <sub>2</sub> .2H <sub>2</sub> O	73.0
Co(CH <sub>3</sub> COO) <sub>2</sub> .4H <sub>2</sub> O	38.0
Co(NO <sub>3</sub> ) <sub>2</sub> .6H <sub>2</sub> O	134.0
CoSO <sub>4</sub> .7H <sub>2</sub> O	36.2
CoCl <sub>2</sub> .6H <sub>2</sub> O	52.9
Ni(CH <sub>3</sub> COO) <sub>2</sub> .4H <sub>2</sub> O	182.0
Ni(NO <sub>3</sub> ) <sub>2</sub> .6H <sub>2</sub> O	238.5
NiSO <sub>4</sub> .7H <sub>2</sub> O	75.6
NiCl <sub>2</sub> .6H <sub>2</sub> O	254.0
Mn(CH <sub>3</sub> COO) <sub>2</sub> .4H <sub>2</sub> O	23.3
Mn(NO <sub>3</sub> ) <sub>2</sub> .4H <sub>2</sub> O	380.0
MnSO <sub>4</sub> .4H <sub>2</sub> O	70.0
MnCl <sub>2</sub> .4H <sub>2</sub> O	198.0

When the solubility values of the metal salts given in Table 2 and 3 are examined, it was determined that the solubility values of the metal cation and the salt compounds formed by the anion with the closest radii are the lowest as expected. However, unlike NO<sub>3</sub><sup>-</sup>, Cl<sup>-</sup> and CH<sub>3</sub>COO<sup>-</sup> anions, all of which have a 1- oxidation step, SO<sub>4</sub><sup>2-</sup> anion, which has a 2- oxidation step, will generate a stronger electron than other anions in order to reduce the electronic stress created by the 2- charge in its structure. For this reason, the solubility of the salt compounds formed by binding to metal cations with ionic bonds with stronger covalent character compared to other anions will be lower than expected.

#### 4. Conclusion

As seen with the anion radius order of the salts from which metal nanopowder is obtained, it is determined that salts with

acetate anion form the smallest particles, although the radius of sulfate is the largest anion, its strong covalent character in binding to metal cations causes a decrease in resolution. As a result, it has been determined that the radii of metal nanopowder obtained by reduction from sulphate anion salts are the largest. This situation can be attributed to the fact that the solubility of metal salts formed by acetate anions with the closest ratio of metal cations and acetate anions is the most difficult and consequently the amount of metal cation obtained as a result of partial dissolution in water is reduced in a controlled manner and transformed into metal nanopowder. It is thought that metal nano powders obtained by reducing metal salts with higher solubility in aqueous environment very quickly with ascorbic acid increase in size as a result of agglomeration.

When the cation radius order of the salts from which the metal nano powders were examined, it was determined that the

average particle size of the nanopowder obtained from Ni<sup>2+</sup> cations with a larger radius compared to the other cations was the smallest, and the radii of the nano metal powders obtained from Co<sup>2+</sup> cation salts with the smallest radius were found to have the largest average. The reason for this is that the particle size of the nano powder obtained from the Ni (CH<sub>3</sub>COO)<sub>2</sub> salt, which has the lowest solubility compared to the anion-cation ratio, is the lowest and the particle size of the nano metal powder obtained from the Co(NO<sub>3</sub>)<sub>2</sub> salt, which has the highest solubility, is the highest. It has been determined that the particle sizes of other nano metal powders change in parallel with the change in the solubility of ionic salts (including exceptional cases).

## References

- [1] F. J. Heiligtag and M. Niederberger, ‘The fascinating world of nanoparticle research’, *Mater. Today*, vol. 16, no. 7–8, pp. 262–271, 2013, doi: 10.1016/j.mattod.2013.07.004.
- [2] M. De, P. S. Ghosh, and V. M. Rotello, ‘Applications of nanoparticles in biology’, *Adv. Mater.*, vol. 20, no. 22, pp. 4225–4241, 2008, doi: 10.1002/adma.200703183.
- [3] S. Shrivastava and D. Dash, ‘Applying Nanotechnology to Human Health: Revolution in Biomedical Sciences’, *J. Nanotechnol.*, vol. 2009, pp. 1–14, 2009, doi: 10.1155/2009/184702.
- [4] S. S. Sana *et al.*, ‘Recent advances in essential oils-based metal nanoparticles: A review on recent developments and biopharmaceutical applications’, *J. Mol. Liq.*, vol. 333, p. 115951, 2021, doi: 10.1016/j.molliq.2021.115951.
- [5] P. Alexandridis and M. Tsianou, ‘Block copolymer-directed metal nanoparticle morphogenesis and organization’, *Eur. Polym. J.*, vol. 47, no. 4, pp. 569–583, 2011, doi: 10.1016/j.eurpolymj.2010.10.021.
- [6] V. Sharma *et al.*, ‘Nanoparticles as Fingerprint Sensors’, *TrAC Trends Anal. Chem.*, vol. 143, p. 116378, 2021, doi: 10.1016/j.trac.2021.116378.
- [7] A. Pawar, S. Thakkar, and M. Misra, ‘A bird’s eye view of nanoparticles prepared by electro spraying: advancements in drug delivery field’, *J. Control. Release*, vol. 286, no. July, pp. 179–200, 2018, doi: 10.1016/j.jconrel.2018.07.036.
- [8] K. McNamara and S. A. M. Tofail, ‘Nanoparticles in biomedical applications’, *Adv. Phys. X*, vol. 2, no. 1, pp. 54–88, 2017, doi: 10.1080/23746149.2016.1254570.
- [9] M. X. Zhao and E. Z. Zeng, ‘Application of functional quantum dot nanoparticles as fluorescence probes in cell labeling and tumor diagnostic imaging’, *Nanoscale Res. Lett.*, vol. 10, no. 1, pp. 1–9, 2015, doi: 10.1186/s11671-015-0873-8.
- [10] M. Zargar *et al.*, ‘Green synthesis and antibacterial effect of silver nanoparticles using *Vitex negundo* L.’, *Molecules*, vol. 16, no. 8, pp. 6667–6676, 2011, doi: 10.3390/molecules16086667.
- [11] G. Yang *et al.*, ‘Understanding the relationship between particle size and ultrasonic treatment during the synthesis of metal nanoparticles’, *Ultrason. Sonochem.*, vol. 73, p. 105497, 2021, doi: 10.1016/j.ultsonch.2021.105497.
- [12] Q. Zhang, Y. Zhang, Y. Li, P. Ding, S. Xu, and J. Cao, ‘Green synthesis of magnetite nanoparticle and its regulatory effect on fermentative hydrogen production from lignocellulosic hydrolysate by *Klebsiella* sp.’, *Int. J. Hydrogen Energy*, vol. 46, no. 39, pp. 20413–20424, 2021, doi: 10.1016/j.ijhydene.2021.03.142.
- [13] K. Fukuda *et al.*, ‘Exfoliated nanosheet crystallite of cesium tungstate with 2D pyrochlore structure: Synthesis, characterization, and photochromic properties’, *ACS Nano*, vol. 2, no. 8, pp. 1689–1695, 2008, doi: 10.1021/nm800184w.
- [14] U. Nithiyantham, S. R. Ede, S. Anantharaj, and S. Kundu, ‘Self-assembled NiWO<sub>4</sub> nanoparticles into chain-like aggregates on DNA scaffold with pronounced catalytic and supercapacitor activities’, *Cryst. Growth Des.*, vol. 15, no. 2, pp. 673–686, 2015, doi: 10.1021/cg501366d.
- [15] L. Zhang, Y. Man, and Y. Zhu, ‘Effects of Mo replacement on the structure and visible-light-induced photocatalytic performances of Bi<sub>2</sub>WO<sub>6</sub> photocatalyst’, *ACS Catal.*, vol. 1, no. 8, pp. 841–848, 2011, doi: 10.1021/cs200155z.
- [16] H. Eranjaneya and G. T. Chandrappa, ‘Solution Combustion Synthesis of Nano ZnWO<sub>4</sub> Photocatalyst’, *Trans. Indian Ceram. Soc.*, vol. 75, no. 2, pp. 133–137, 2016, doi: 10.1080/0371750X.2016.1181990.
- [17] E. C. Dreaden, A. M. Alkilany, X. Huang, C. J. Murphy, and M. A. El-Sayed, ‘The golden age: Gold nanoparticles for biomedicine’, *Chem. Soc. Rev.*, vol. 41, no. 7, pp. 2740–2779, 2012, doi: 10.1039/c1cs15237h.
- [18] A. Ali *et al.*, ‘Synthesis, characterization, applications, and challenges of iron oxide nanoparticles’, *Nanotechnol. Sci. Appl.*, vol. 9, pp. 49–67, 2016, doi: 10.2147/NSA.S99986.
- [19] R. A. Ismail, S. A. Zaidan, and R. M. Kadhim, ‘Preparation and characterization of aluminum oxide nanoparticles by laser ablation in liquid as passivating and anti-reflection coating for silicon photodiodes’, *Appl. Nanosci.*, vol. 7, no. 7, pp. 477–487, 2017, doi: 10.1007/s13204-017-0580-0.

- [20] W. M. M. Mahmoud, T. Rastogi, and K. Kümmerer, 'Application of titanium dioxide nanoparticles as a photocatalyst for the removal of micropollutants such as pharmaceuticals from water', *Curr. Opin. Green Sustain. Chem.*, vol. 6, pp. 1–10, 2017, doi: 10.1016/j.cogsc.2017.04.001.
- [21] M. O. Amin, M. Madkour, and E. Al-Hetlani, 'Metal oxide nanoparticles for latent fingerprint visualization and analysis of small drug molecules using surface-assisted laser desorption/ionization mass spectrometry', *Anal. Bioanal. Chem.*, vol. 410, no. 20, pp. 4815–4827, 2018, doi: 10.1007/s00216-018-1119-2.
- [22] N. Krishna, G. N. Kumar, T. Neethu, R. John, S. R. Babu, and S. Smitha Chandran, 'One Pot Green Synthesis of Silver Nanoparticles with Multiple Applications', *Mater. Today Proc.*, vol. 5, no. 9, pp. 20567–20571, 2018, doi: 10.1016/j.matpr.2018.06.435.
- [23] A.T.A. Ibrahim, 'Toxicological impact of green synthesized silver nanoparticles and protective role of different selenium type on *Oreochromis niloticus*: hematological and biochemical response', *J. Trace Elem. Med. Biol.*, vol. 61, no. November 2019, p. 126507, 2020, doi: 10.1016/j.jtemb.2020.126507.
- [24] S. P. Chandran, M. Chaudhary, R. Pasricha, A. Ahmad, and M. Sastry, 'Synthesis of gold nanotriangles and silver nanoparticles using Aloe vera plant extract', *Biotechnol. Prog.*, vol. 22, no. 2, pp. 577–583, 2006, doi: 10.1021/bp0501423.
- [25] P. Rani, L. Trivedi, S. Singh, A. Singh, and G. Shukla, 'Materials Today : Proceedings Green synthesis of silver nanoparticles by *Cassytha filiformis* L . extract and its characterization', *Mater. Today Proc.*, no. xxxx, 2021, doi: 10.1016/j.matpr.2021.07.166.
- [26] A. Umer, S. Naveed, N. Ramzan, and M. S. Rafique, 'Selection of a suitable method for the synthesis of copper nanoparticles', *Nano*, vol. 7, no. 5, 2012, doi: 10.1142/S1793292012300058.
- [27] A. Umer, S. Naveed, N. Ramzan, M. S. Rafique, and M. Imran, 'A green method for the synthesis of copper nanoparticles using l-ascorbic acid', *Rev. Mater.*, vol. 19, no. 3, pp. 197–203, 2014, doi: 10.1590/S1517-70762014000300002.
- [28] L. Malassis, R. Dreyfus, R. J. Murphy, L. A. Hough, B. Donnio, and C. B. Murray, 'One-step green synthesis of gold and silver nanoparticles with ascorbic acid and their versatile surface post-functionalization', *RSC Adv.*, vol. 6, no. 39, pp. 33092–33100, 2016, doi: 10.1039/c6ra00194g.
- [29] D. Dutta and B. M. Das, 'Scope of green nanotechnology towards amalgamation of green chemistry for cleaner environment: A review on synthesis and applications of green nanoparticles', *Environ. Nanotechnology, Monit. Manag.*, vol. 15, no. December 2020, p. 100418, 2021, doi: 10.1016/j.enmm.2020.100418.
- [30] P. Rajiv, B. Bavadharani, M. N. Kumar, and P. Vanathi, 'Synthesis and characterization of biogenic iron oxide nanoparticles using green chemistry approach and evaluating their biological activities', *Biocatal. Agric. Biotechnol.*, vol. 12, no. June, pp. 45–49, 2017, doi: 10.1016/j.bcab.2017.08.015.
- [31] A. De, R. Das, P. Jain, and H. Kaur, 'Green chemistry-assisted synthesis of CuO nanoparticles: Reaction optimization, DNA cleavage, and DNA binding studies', *Mater. Today Proc.*, no. xxxx, pp. 1–4, 2020, doi: 10.1016/j.matpr.2020.10.955.
- [32] T. Naseem and T. Durrani, 'The role of some important metal oxide nanoparticles for wastewater and antibacterial applications: A review', *Environ. Chem. Ecotoxicol.*, vol. 3, pp. 59–75, 2021, doi: 10.1016/j.enceco.2020.12.001.
- [33] H. D. B. Jenkins and K. P. Thakur, 'Reappraisal of thermochemical radii for complex ions', *J. Chem. Educ.*, vol. 56, no. 9, pp. 576–577, 1979, doi: 10.1021/ed056p576.
- [34] R.D. Shannon, 'Revised effective ionic radii and systematic studies of interatomic distances in halides and chalcogenides', *Acta Cryst.*, vol. A, no. 32, pp. 751–767, 1976, doi: 10.1107/S0567739476001551.